

# RECENT PROGRESS ON SLED, THE SLAC ENERGY DOUBLER\*

Z. D. Farkas, H. A. Hogg, G. A. Loew, P. B. Wilson

Stanford Linear Accelerator Center  
Stanford, California, 94305

## Introduction

The recent discovery of  $\psi$  particles has added further incentive to the search for ways of increasing the beam energy at SLAC. Several schemes for achieving higher energies have been explored in recent years. The system described here, which has become known as SLED (SLAC Energy Doubler), has now received ERDA approval for gradual installation, using Accelerator Improvement Funds.

As presently conceived, SLED has the advantage that it will not increase the average power consumed by the accelerator, and is therefore compatible with national energy-conservation goals. Peak RF power will be enhanced at the expense of RF pulse length, so that the accelerator will deliver shorter pulses of higher-energy electrons with a duty cycle a factor of ten lower than at present.

From the following description, it will be seen that SLED raises the accelerator peak energy by 40% if the present 2.7  $\mu$ s RF pulse length is used. The energy increase is 80% if the pulse length is extended to 5  $\mu$ s. To do this, however, changes have to be made in the modulators and trigger system, and the maximum repetition rate has to be halved to maintain the present average power level. In addition, more extensive switchyard modifications are required for handling the higher energy beams. For these reasons, the SLED system will be initially installed and run at the present 2.7  $\mu$ s pulse length. Performance at both pulse lengths is discussed in this paper.

## Description of Operating Principles

In essence, SLED is a novel method of achieving RF pulse-compression through the use of high-Q resonant cavities. The cavities store klystron energy during a large fraction of each pulse and then discharge this energy rapidly into the accelerator during the remainder of the pulse.

A development of the equations governing cavity and accelerator performance can be found in Ref. 1.

As a basis for comparison, Fig. 1a shows schematically how, in the present SLAC accelerator, a 2.7  $\mu$ s RF pulse is transmitted directly from the klystrons into the accelerating sections. Fig. 1b shows the SLED modification. A 3-dB sidewall waveguide coupler is inserted into the waveguide leading from the klystron to the accelerator. Two identical cavities, resonant at the SLAC RF frequency (2.856 GHz), are connected to the remaining coupler ports as shown. A fast-acting triggered PIN diode  $\pi$ -phase-shifter is inserted into the klystron drive-line. The output waveform is shown for the case of the longer (5  $\mu$ s) RF pulse. The following is a description of the process by which the output waveform is generated:

(1) A small part of the klystron power is used to build up RF fields inside the cavities. The balance of the klystron power is reflected from the waveguide/cavity interface. As a consequence of the  $\pi/2$  phase-shift imparted to waves crossing the coupler slot, all of this power is transmitted to the accelerator, and none is returned to the klystron. Fig. 1b shows the klystron waveform  $E_K$  incident upon the cavities and Fig. 2a shows the transmitted waveform  $E_T$  leaving the cavities. We assume  $|E_T| \approx |E_K| = 1$ .

(2) Energy stored in the cavities re-radiates an RF wave (the emitted wave  $E_e$ ) which travels to the accelerator exactly out of phase with the transmitted klystron wave  $E_T$ .

The field  $E_L$  at the input to the accelerator is due to the sum of these two waves, i.e.,

$$E_L = E_e + E_T \quad (1)$$

Again, the coupler phase-shift characteristics are such that no emitted power is returned to the klystron. The waveforms of  $E_e$  and  $E_L$  are plotted in Figs. 2b and 2c respectively. It is seen that Fig. 2 is divided into three time intervals: A ( $0 < t < t_1$ ), B ( $t_1 < t < t_2$ ) and C ( $t > t_2$ ). In the time interval A,

$$E_e(A) = \alpha [1 - e^{-\tau}] \quad (2)$$

where

$$\alpha = 2\beta/(1 + \beta)$$

$$\beta = \text{cavity coupling coefficient}$$

$$\tau = t/T_c$$

$$T_c = \text{cavity filling time} = 2Q_L/\omega$$

$$\omega = \text{radian frequency}$$

$$Q_L = Q_0/(1 + \beta)$$

$$Q_0 = \text{cavity unloaded quality factor}$$

Thus, in time interval A,

$$E_L(A) = E_e(A) - 1 = \alpha [1 - e^{-\tau}] - 1 \quad (3)$$

If the cavities are overcoupled ( $\beta > 1$ ),  $E_e$  grows in time to an amplitude greater than  $E_T$ , and  $E_L$  goes through a phase reversal, as shown.

(3) The charging cycle is terminated at time  $t_1$  by reversing the phase of the klystron RF very rapidly (compared to the filling-time of the cavities). The emitted and transmitted waves then add, producing a surge of high power into the accelerator. It is clear that if  $\beta$  and  $\tau_1 (= t_1/T_c)$  are large,  $E_e$  approaches a value of  $\alpha = +2$  and  $E_L$  approaches +1. Thus, upon phase reversal,  $E_T$  changes from -1 to +1 and  $E_L$  jumps from +1 to +3, giving an instantaneous power multiplication of 9.

Following the phase reversal,  $E_e$  decreases rapidly as the cavities try to charge up to a new field level of opposite phase. In time interval B,

$$E_e(B) = \gamma e^{-(\tau - \tau_1)} - \alpha \quad (4)$$

and

$$E_L(B) = E_e(B) + 1 = [\gamma e^{-(\tau - \tau_1)} - \alpha] + 1 \quad (5)$$

where

$$\gamma = \alpha(2 - e^{-\tau_1})$$

(4) At the end of the klystron pulse at time  $t_2$  (one accelerator filling time after the phase reversal),  $E_T$  drops to zero. Thus, in time interval C,

$$E_L(C) = E_e(C) = [\gamma e^{-(\tau_2 - \tau_1)} - \alpha] e^{-(\tau - \tau_2)} \quad (6)$$

The waveforms in Fig. 2 are plotted for  $\beta = 5$ ,  $\tau_1 = 2$  and  $\tau_2 = 2.4$ , which are values of practical interest at SLAC. Fig. 2d illustrates the SLED energy gain imparted to an electron passing through the accelerator. The gain is shown as a function of time through the RF pulse and is normalized to

\* Work supported by U. S. Energy Research and Development Administration.

the acceleration obtained (after one filling time) from a standard flat-topped pulse of amplitude  $E_K = 1$ . A constant-gradient accelerating structure of length  $L$  is assumed, in which the group velocity varies linearly with distance  $z$  along the structure according to  $v_g(z) = v_{g0}(1 - gz/L)$ . Analytic expressions are derived in Ref. 1. Here we give just the expression for maximum energy, which is obtained at  $t = t_2$ , one accelerator filling-time  $T_a$  after phase reversal:

$$V_{\max} = M = e^{-T_a/T_c} \left[ 1 - (1 - g)^{1+\nu} \right] \left[ g(1+\nu) \right]^{-1} - (\alpha - 1) \quad (7)$$

where

$$\nu = (T_a/T_c) \left[ \ln(1 - g) \right]^{-1}.$$

It is clear that the no-load energy variation around the peak is large, resulting in a poor spectrum even for very narrow beam pulses. However, at high current levels, the transient beam-loading characteristic of the accelerator structure can be utilized to provide energy compensation. The beam, which has a pulse width  $T_b$ , is injected at time  $(t_2 - T_b)$  so that it ends at the instant of maximum no-load energy. The beam current is adjusted so that at  $t_2$ , beam loading just cancels the rise in SLED energy during  $T_b$ . Of course, cancellation at intermediate times is imperfect because the curves don't match. First-order curve-matching can be done by starting with a high current beam and stepping to a lower current about half-way through the pulse. It is calculated that spectrum widths of 0.5% can be obtained in this way at the 10% beam-loading level, at average beam currents of 14  $\mu A$ . The beam pulse width  $T_b$  is 250 ns (360 pps) with a 2.7  $\mu s$  klystron pulse, and 350 ns (180 pps) with a 5  $\mu s$  klystron pulse. For comparison, the present SLAC average current at 10% beam loading is 40  $\mu A$ .

At lower currents, the energy spectrum may be narrowed by advancing the phase-reversal time,  $t_1$ , on an appropriate number of klystrons. Advancing  $t_1$  also advances the time of maximum energy and decreases its amplitude (because the cavity charging time is reduced). As the peak SLED fields propagate out of the accelerator section, the energy decreases almost linearly until time  $t_2$ , when the energy begins to fall off more rapidly as the accelerator section empties. Thus, on those stations where  $t_1$  is advanced by  $T_b$ , the energy contribution decreases almost linearly through the beam time. This characteristic can be used in the same manner as beam-loading for energy compensation. By selecting the optimum mix of "advanced" and "normal" SLED stations, it should be possible to produce acceptably narrow spectra at any beam current.

### SLED Cavity Design

Technological and economic boundary conditions have made the selection of SLED cavity parameters relatively simple. For instance, the existing klystron modulator power supplies (and the technology of pulse-transformer design) limit the RF pulse length to 5  $\mu s$ . The use of superconducting RF cavities was ruled out by budget considerations, so a working value of  $Q_0 = 10^5$ , which can be obtained with room-temperature copper cavities, has been assumed. Analysis of Eq. (7) then indicates that  $\beta$  should lie between 4 and 5 to maximize the energy multiplication factor  $M$  under these conditions.

Considerations of cost, mechanical stability and mode separation make it desirable to choose a mode which, for a given  $Q_0$ , has close to minimum volume. Various members of the  $TE_{0mn}$  family were considered and the  $TE_{015}$  was finally selected. A diameter (D)-to-length (L) ratio of 0.611 was chosen to maximize frequency separation between competing modes. The actual cavity dimensions are  $D = 20.51$  cm and  $L = 33.59$  cm. The calculated  $Q_0$  for copper construction is  $1.08 \times 10^5$ .

Clearly, there are mechanical and temperature tolerances to be concerned with. The tuning rates for changes in cavity diameter and length are both approximately  $-5.3$  kHz/ $\mu$ m. The cavity tuning angle  $\psi$  is defined by  $\psi = \arctan 2Q_L \Delta f/f$ , where  $\Delta f$  is the difference between the cavity resonant frequency and the generator frequency  $f$  and  $\Delta f/f$  is equal to  $k\Delta T$ , where  $k$  is the linear coefficient of thermal expansion and  $T$  is the temperature. Taking  $Q_L = 1.8 \times 10^4$  gives  $\Delta\psi/\Delta T = 31^\circ/\text{C}$  for copper cavities. It is calculated that, when  $\psi = 10^\circ$ , the maximum beam energy,  $V_{\max}$ , is decreased by 1%. Phase shift and amplitude reduction contribute approximately equally to this energy decrease. The existing accelerator water cooling system is stable to  $\pm 0.15^\circ\text{C}$ , which implies that  $\psi$  can be held to  $\pm 5^\circ$ . However, calculations indicate that the RF power dissipation inside a cavity (assuming 30 MW peak klystron power, 27 kW average power and 1.6 l/s cooling water flow per cavity) will raise the average metal temperature by  $1.4^\circ\text{C}$ . Thus, although each set of cavities could be tuned for SLED operation at the normal power level of the klystron attached to it, the cavities would be proportionately mistuned at other power levels and repetition rates. In particular, when changing from non-SLED to SLED operation, the initial mis-tuning could be up to 1/4 of a bandwidth. Thus, a short warm-up period would be required for the cavities to come to resonance. However, our first measurements indicate that, while the metal temperature excursions are close to predictions, the cavity-field phase-and-amplitude-shifts are much smaller than expected.

Two SLED assemblies have been built and tested so far. Both have substantially the same microwave design, but the second assembly incorporates many mechanical refinements as a result of experience with the first. Cavities and 3-dB couplers are made from OFHC copper. Surface finish inside the cavities is better than 0.15  $\mu\text{m}$  RMS. Measurements are being made to determine how much the surface finish requirement can be relaxed without spoiling the Q.

The cavities are mounted side-by-side in a stainless-steel framework. The 3-dB coupler is supported by an extension of the framework. Coupler and cavities are connected by waveguide "dog-legs" which are brazed into the cavity end-plates. Circular apertures in the end-plates allow strong magnetic coupling between the waveguide and cavity fields. The other end-plate of each cavity incorporates a stiff diaphragm which can be moved by a differential-screw mechanism for fine-tuning.

In order to return to the standard SLAC acceleration mode with flat-topped RF pulses, it is necessary to detune the cavities, which then present identical reactances to the 3-dB coupler ports. Detuning is achieved by inserting tungsten needles into the cavities. Each needle enters its cavity through a hole drilled on a current nodal circle. The needle is slanted so that when it is fully inserted, its tip reaches a circle of maximum azimuthal electric field. Adequate detuning (about 100 bandwidths) is readily achieved, and the cavities return accurately to resonance when the needles are retracted and equilibrium temperature is re-established. The needles are attached to steel armatures which slide in guide tubes attached to the cavities. A permanent magnet is fitted over each guide tube, external to the vacuum system. As the magnet is moved, its field pulls the armature, and hence the needle, along with it.

The input and output ports of the 3-dB coupler, which are connected to the klystron and the waveguide leading to the accelerator, respectively, have loop-type dual-directional couplers for signal monitoring. Also, there are coupling loops in each cavity which are used for tuning to exact resonance at the machine frequency.

### Experimental Results

The first SLED assembly was baked-out and high-

power tested in the laboratory before being installed on the machine. The output power was fed directly into a load, which gave problems due to breakdown at very high powers. Nevertheless, operation at 140 MW peak SLED power was eventually reached. At this level, the klystron was running at 25 MW, 60 pps, 5  $\mu$ s pulse-length.

The installation was then moved to Station 1-1C at the beginning of the SLAC accelerator. This station feeds a single accelerator section which is immediately followed by a momentum analyzer. Measurements were begun with the standard 2.7  $\mu$ s pulse length. After some initial load breakdown, stable operation at 14-MW klystron peak power (58-MW SLED peak) was achieved. Thus, the ability of one accelerator section and its load to handle the maximum anticipated SLED peak power has already been demonstrated. (We assume a 40-MW klystron, 5- $\mu$ s pulse length, 7.7 dB SLED gain and subsequent power division between four accelerator sections.) The SLED power gain at this pulse length was 6.2 dB; close to theoretical (6.3 dB).

Probing the SLED beam energy multiplication factor as a function of time through the RF pulse was done by injecting a 80 ns-wide beam pulse into Section 1-1C and running it into the momentum analyzer. Differential energy measurements at 100 ns time intervals were reduced to give the data points plotted in Fig. 3. It is seen that there is very good agreement with the theoretical curve.

Measurements were then extended to 5  $\mu$ s pulses. The increased klystron pulse length necessitated several machine changes which made the experiment more difficult to set up and run. First, the modulator PFN had to be lengthened. (The klystron had previously been fitted with a redesigned pulse transformer to handle the longer pulse length). Then the standby sub-booster for the machine had to be modified to provide a 5  $\mu$ s drive signal. Finally, variable delays were inserted in the injector trigger system so that the beam timing could be moved through the long RF pulse.

Gas bursts and load-arcing were initially experienced as the SLED peak power was raised. However, the system cleaned up and stabilized after a number of hours of running.

The first tests yielded a power gain of 7.2 dB, and beam momentum analysis indicated a peak SLED energy multiplication factor of 1.67. Theoretical and experimental energy curves are presented for comparison in Fig. 4. It is seen that the measured values are somewhat less than predicted. The cavities were found to have become mistuned, presumably due to mechanical stresses. After retuning, the gain increased to 7.6 dB. Machine scheduling did not permit the beam energy test to be re-run at that time. The output waveform obtained with a 5  $\mu$ s, 12 MW input pulse is shown in Fig. 5. The peak power is 70 MW.

The second prototype SLED assembly has been installed with a 30 MW klystron at Station 1-8, as shown in Fig. 7. No momentum analyzer is available near this location for beam energy measurements. The station was chosen because it has the standard SLAC four-way power division to four accelerator sections and, in addition, it can still be conveniently driven by the standby sub-booster, mentioned earlier. Tests to date have been limited to 2.7  $\mu$ s RF pulse length. Operation at 30 MW, 360 pps has been readily achieved. The output waveform at this level is shown in Fig. 6. The SLED peak power is 125 MW. As mentioned

earlier, the system gain-and phase-stability as a function of internal RF power dissipation is better than predicted. For instance,  $\Delta\phi/\Delta T$  appears to be nearer 8°/°C. However, there are small tuning changes which correlate with ambient temperature fluctuations. The causes for these are being identified. Tests at 5  $\mu$ s pulse length will be started shortly.

At the present time, the SLED program appears technically feasible and operationally promising. It is planned to equip two sectors with SLED assemblies (16 pairs of cavities) by the end of this year. If their performance is satisfactory, installation will continue at an accelerated pace, aiming at complete machine conversion by the end of 1977.

#### Acknowledgements

It is a pleasure to acknowledge the continuing support and encouragement of many SLAC groups and individuals. The Klystron Department under J. Lebacqz, has helped in many ways - with special tubes, components, instrumentation and personnel. C. Olsen's Accelerator Electronics Department has worked on the long-pulse modulators. A. Lisin and R. Sandkuhle, assisted by R. Laurie, have done an excellent job on the SLED mechanical design. H. Zaiss' Mechanical Fabrication Department has been responsible for all machining and brazing. H. Deruyter has done excellent work on all the low-and high-power microwave testing.

#### References

1. Z.D. Farkas, *et al.*, "SLED: A Method of Doubling SLAC's Energy," Proc. 9th Int. Conf. on High Energy Accelerators, SLAC, Stanford, California, May 2 - 7, 1974, p.576.

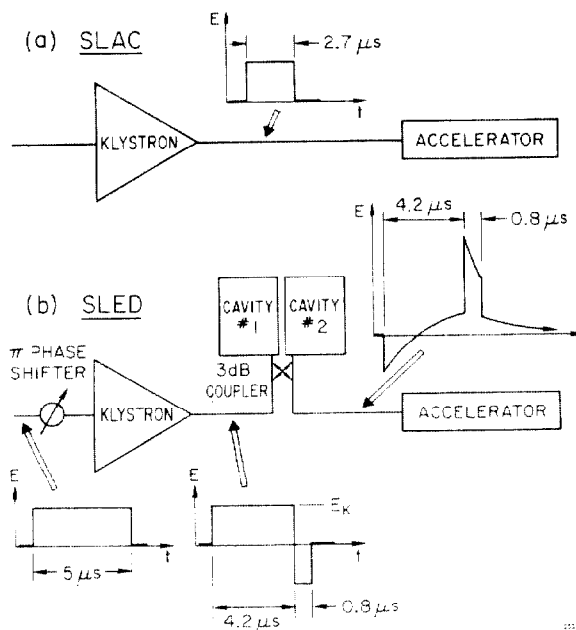


FIG. 1--A comparison of the SLAC and SLED RF systems.

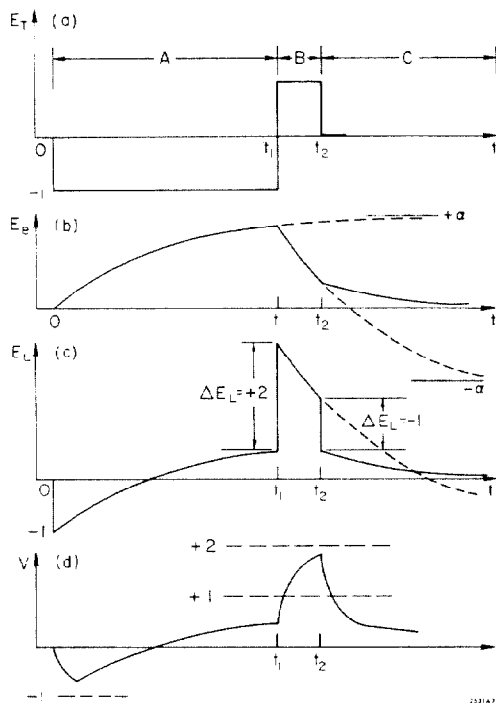


FIG. 2--SLED waveforms.

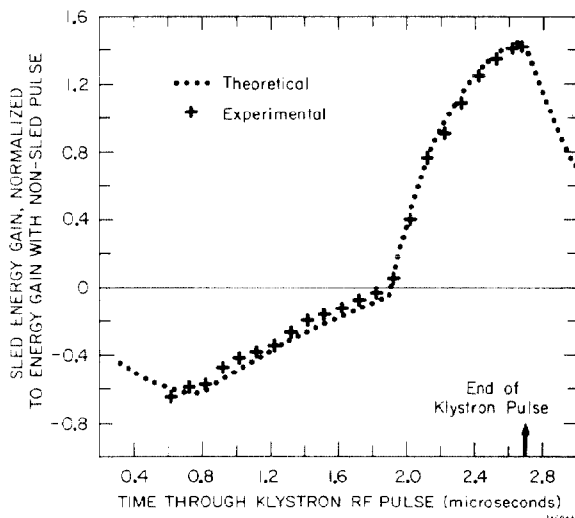


FIG. 3--Normalized SLED energy gain for a 2.7  $\mu$ s RF pulse.

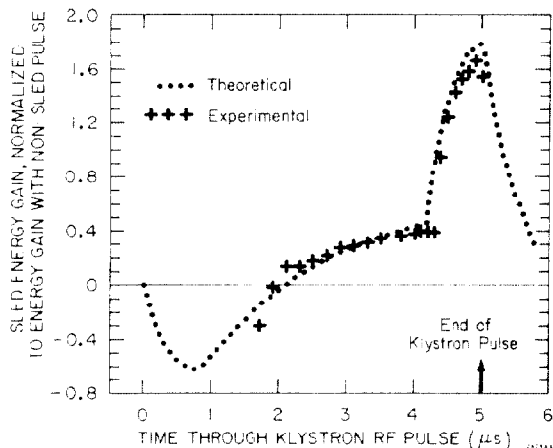


FIG. 4--Normalized SLED energy gain for a 5.0  $\mu$ s RF pulse.

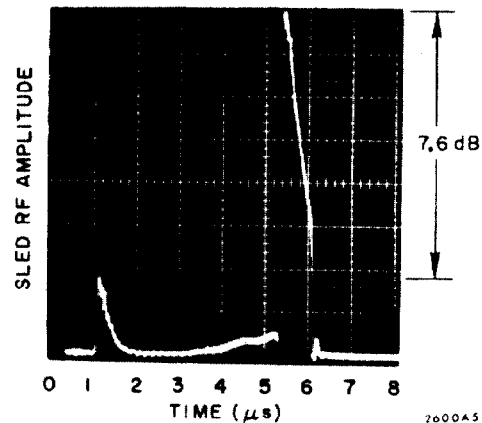


FIG. 5--SLED output waveform generated by a 5  $\mu$ s, 12 MW input pulse. Peak output to accelerator is 70 MW.

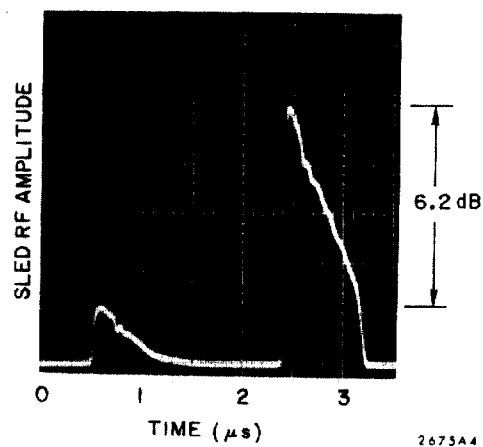


FIG. 6--SLED output waveform generated by a 2.7  $\mu$ s, 30 MW input pulse. Peak output to accelerator is 125 MW.

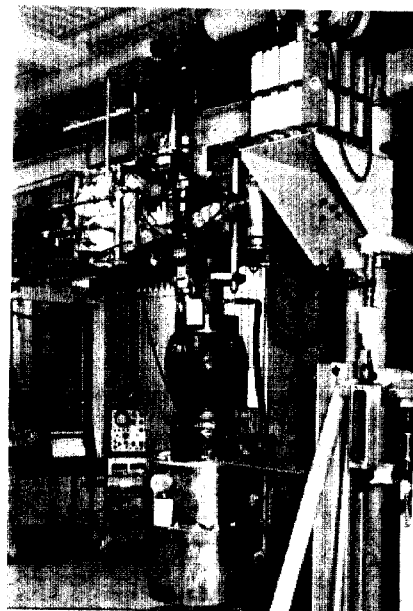


FIG. 7--View of second SLED prototype installation in klystron gallery.